Article:
Inam, A, Brydson, R orcid.org/0000-0003-2003-7612 and Edmonds, DV (2020) Raman spectroscopy study of the crystallinity of graphite formed in an experimental free-machining steel. Materials Characterization, 163. 110264. ISSN 1044-5803

https://doi.org/10.1016/j.matchar.2020.110264

Raman Spectroscopy Study of the Crystallinity of Graphite Formed in an Experimental Free-Machining Steel

A. Inam [a], R. Brydson [b] and D.V. Edmonds [c]

[a] Department of Metallurgy and Materials Engineering
College of Engineering and Emerging Technologies
University of the Punjab
Quaid-e-Azam Campus
Lahore 54590
Pakistan

[b,c] School of Chemical and Process Engineering
University of Leeds
Leeds, LS2 9JT
United Kingdom

Author email addresses: Aqil Inam [aqil.ceet@pu.edu.pk]; Rik Brydson [mtlrmdb@leeds.ac.uk]; David Edmonds [d.v.edmonds@leeds.ac.uk]

Corresponding Author:

David V Edmonds FREng FIMMM CEng CSci FASM

Professor Emeritus

School of Chemical and Process Engineering

University of Leeds

Leeds LS2 9JT

United Kingdom

email: d.v.edmonds@leeds.ac.uk

Abstract

Appropriate graphitisation of a carbon steel may provide an alternative route to developing more simply and inexpensively alloyed machining steels which are more recyclable than those which are currently available. The extent of crystallinity of graphite particles formed during a graphitisation anneal of an experimental carbon steel was studied by Raman spectroscopy. It is demonstrated that it was possible to record the progress of graphitisation

with annealing time as well as to determine which starting microstructural conditions, either ferrite-pearlite, bainite or martensite, formed the most highly crystalline graphite particles during annealing. During a machining operation the graphite should act as an internal lubricant at the chip/tool interface and thus the extent of crystallinity may influence the final machinability of the steel, or effectively, optimisation of the heat treatment. It was revealed by the Raman spectra that the crystallinity of the graphite particles formed was strongly affected by the starting microstructures as well as the graphitising anneal periods. For a similar annealing time, a better degree of crystallinity was observed in graphite particles formed from a ferrite-pearlite starting microstructure rather than bainite and martensite starting microstructures. However, crystallinity could be gradually improved with increasing annealing time from all three of the starting microstructures examined.

Keywords: Raman Spectrometry, Carbon Steel, Machinability, Graphitization, Crystallinity.

1. Introduction

Free cutting steels are used in various industries for the mass production of parts by CNC machines. Existing free cutting steels contain elements e.g. Pb, S, P, Se, Bi, Te, added to improve machinability. Some of these elements are expensive, toxic in chemical nature and they can also make the steels more difficult to recycle [e.g.1-4]. A potential alternative route to improve carbon steel for machining that is being explored [1,5-13] is to avoid extensive alloying by using carbon itself, already in the steel, and which is also a comparatively cheap element. This may be achievable by inducing carbon to form in its free state in the steel, as graphite, rather than in its more usual form which is combined with iron as a carbide (θ-Fe_3C, cementite). This may be achieved by an alternative, and potentially simpler alloying strategy. Cementite is generally a hard brittle phase in steel, often reducing mechanical properties and hence, in the present context, increasing wear of the machine tools and also making industrial forming processes such as forging more difficult [1,14]. In contrast, graphite can act as a solid internal lubricant at the tool-chip interface.

Currently we can consider two acknowledged methods of graphitisation: (1) Destabilisation of cementite by enhancing Si and Al alloying [5-13] and avoiding carbide stabilizing elements such as Mn and Cr [e.g. 15-17]; (2) Providing heterogeneous nucleation sites for graphite using carbides, nitrides and oxides [15], for example, Al_2O_3, AlN, BN, SiO_2,TiC,

ZrN, Nb(C,N), V(C,N), ZrC [18] and Mo_2C [19]. Given that the latter method involves more complex alloying and invariably the use of hard phases, the present work contributes towards the first approach, to understand better the phase behaviour during destabilisation of cementite to form graphite by control of the balance between graphite and carbide forming alloying elements, including, importantly, those normally already present in modern carbon steels, such as Si and Mn.

This study using Raman spectroscopy was carried out to determine the extent of crystallinity of the graphite particles formed during a high temperature graphitising anneal of a simply alloyed experimental carbon steel. As part of the programme the steel was annealed in three starting microstructural conditions: ferrite-pearlite, bainite and martensite.

2. Experimental

A medium carbon experimental steel with composition (wt.%) 0.39C-0.11Mn-1.86Si-1.38Al-0.01P-0.002S was prepared by Tata Steel, Rotherham, UK, as a 60Kg melt hot-rolled to 12 mm thick plates.

Heat treatment produced three pre-anneal starting microstructural conditions:

• Martensite (austenitised 1150 °C for 7 min and water quenched);

• Bainite (austenitised 1150 °C for 7 min and austempered at 400–420 °C for 60 min in a nitrate salt bath);

• Ferrite/pearlite (as-received in the hot-rolled condition).

Graphitising heat-treatments were carried out in a resistance heating furnace; samples were heated to 680 °C at a heating rate ~5 °C/min and annealed for different time periods (~20-300 min) prior to cooling at a rate ~0.5 °C/min to ambient temperature. Following heat treatment specimens were prepared for microstructural study by light optical, electron microscopy and Raman spectroscopy. For microscopic analysis specimens were prepared by metallographic procedures according to the ASTM E3 standard before etching in 2% Nital. The light optical microstructural study was carried out using an Olympus BX51 microscope

with digital micrographs recorded by an Axio Cam MRc 5 (Carl Zeiss) camera. Specimens prepared for light optical microscopy were also used for secondary electron (SE) imaging at 10 kV on a LEO 1530 Gemini FEGSEM equipped with an energy dispersive X-ray (EDX) Silicon Drift Detector (SDD).

A Renishaw Raman spectrometer with a Leica optical microscope and 50x (N.A. = 0.75) objective attached was used for the study of crystallinity of graphite particles. The spectrometer had an argon ion laser of wavelength 514.5 nm and was used at an operating power of 50 mW.

Figure 1 shows graphite particles using the attached light optical microscope. The laser beam can be focused on the central graphite particle to collect a Raman spectrum.

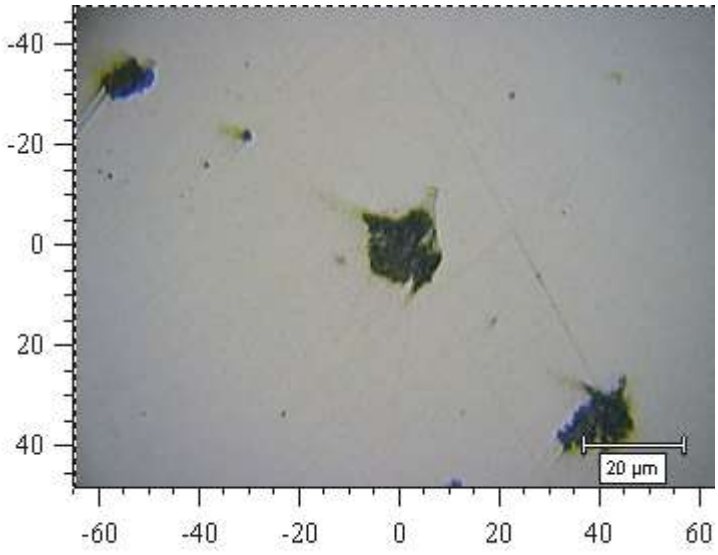

Figure 1 A micrograph taken using the Raman attached optical microscope showing graphite particles (formed from a ferrite-pearlite starting microstructure after 5 hours of graphitising anneal).

Raman spectra from the coarser graphite particles were obtained relatively easily, but those from fine graphite particles with a size $\leq$ 2 µm diameter (formed generally from the martensite starting microstructure) were much more difficult to obtain, since the spot size of the laser beam of the Raman spectrometer has a diameter ~2 µm. Focusing this small laser

beam on small graphite particles was found to be challenging with a manually controlled stage.

3. Results and Discussion

Figure 2 shows SEM micrographs typical of the starting microstructures, ferrite-pearlite, bainite, and martensite, respectively. These background microstructures in the same experimental carbon steel and their detailed transformation during the graphitisation annealing process, including the identification and formation of the graphite particles, have previously been studied in detail by light optical, and scanning and high resolution electron microscopy [5-13]. The present work complements this earlier work by focusing solely upon the behaviour of the graphite particles themselves during annealing.

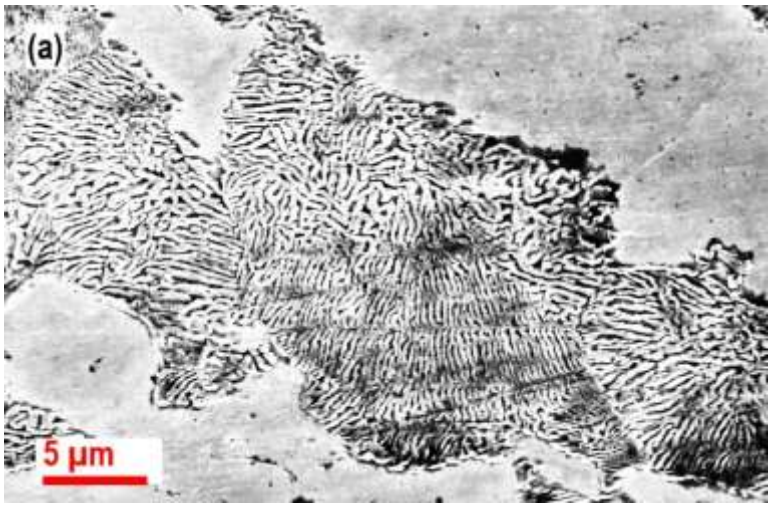

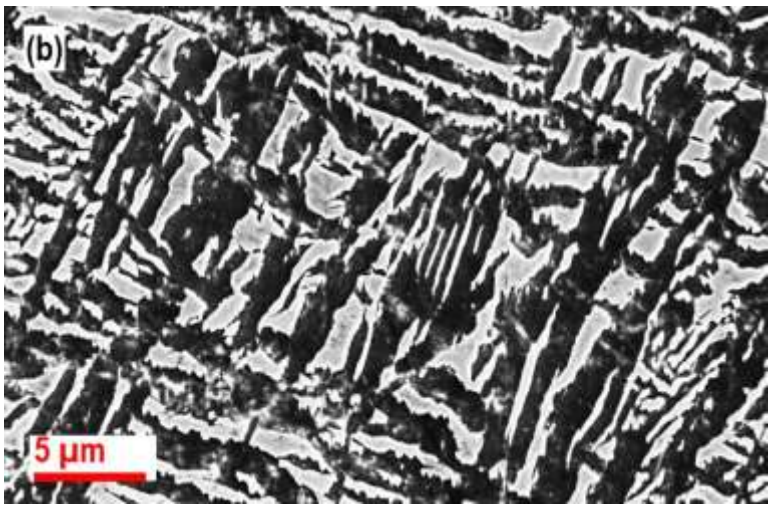

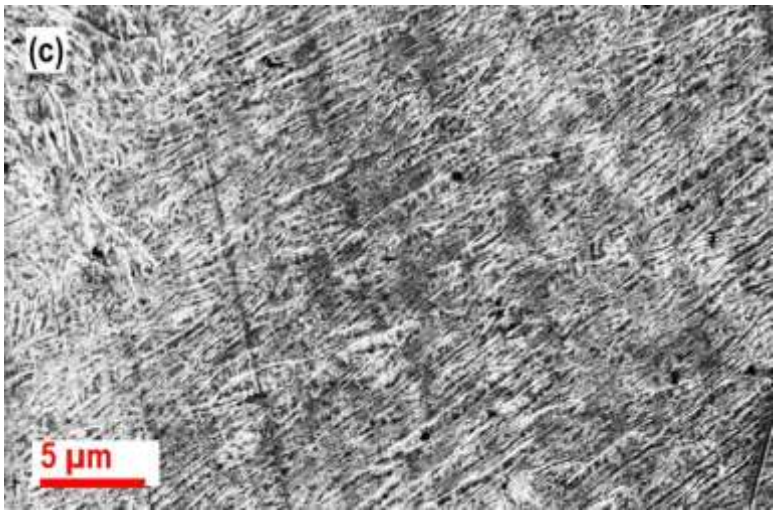

Figure 2 SEM micrographs of etched starting microstructures: (a) ferrite-pearlite, (b) bainite, and (c) martensite.

Figure 3 shows SEM micrographs illustrating typical graphite dispersions of different size and spatial distribution formed from the ferrite-pearlite, bainite, and martensite starting microstructures (as shown in Fig. 2) following 180 minutes of graphitising anneal at 680 °C.

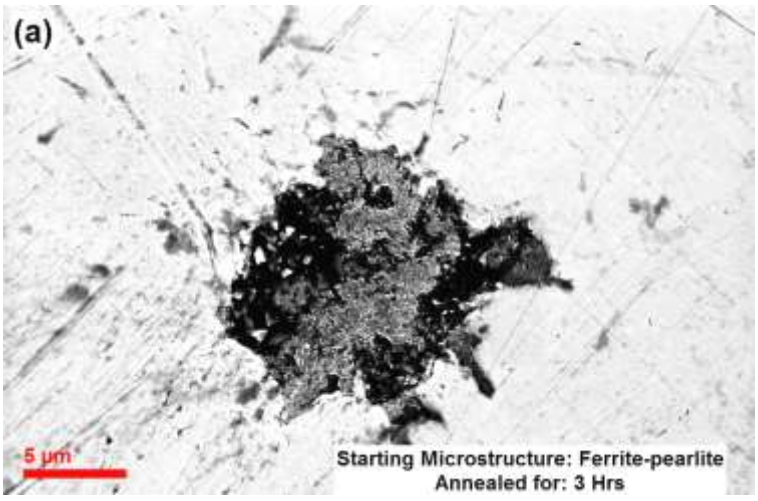

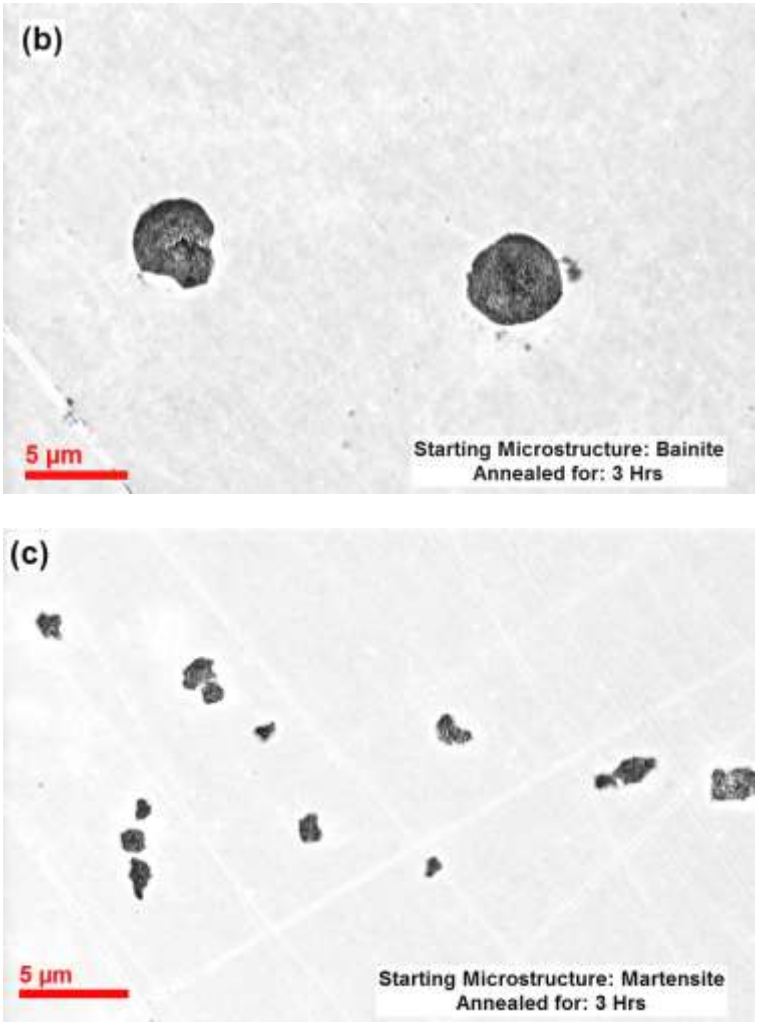

Figure 3. SEM micrographs showing graphite dispersions formed from starting microstructures after a graphitising anneal of 180 minutes at 680 °C: (a) ferrite-pearlite (b) bainite and (c) martensite. (The micrographs were obtained from un-etched samples.)

The approximate size of graphite particles formed after a graphitising anneal in each of the three starting microstructures was ≤ 20, ≤ 5 and ≤ 2 µm from ferrite-pearlite, bainite and martensite, respectively, as reported by Inam et al. [8-12].

A typical Raman spectrum for the central graphite particle in Fig. 1 is shown in Figure 4. As recorded already, this graphite particle was formed in a ferrite-pearlite starting microstructure after 5 hours of graphitising anneal. The figure indicates the intensities and wave numbers (cm^{-1}) of *D*, *G*, *D'* and *G'* bands related to graphite in the Raman spectrum.

As discussed, for example, by Wang and Allred [20] the formation of two characteristic bands, *D* at ≈1350 cm^{-1} and *G* at ≈1590 cm^{-1} in the Raman spectra shows the presence of graphitic carbon. In the Raman spectrum of a single crystal of graphite, the *G* band is

observed at 1580 cm^{-1}. The *G* band is related to first-order phonon scattering, as expected in sp2 carbon, and represents the presence of crystalline graphite, whilst the *D* band arises from a translational-symmetry breaking mode, which is related to the presence of defects, grain boundaries, functional groups or structural disorder and indicates a defective or disordered form of graphite e.g. at the edges of graphite flakes [21]. In graphitic carbons a prominent Raman band is also formed via a second-order double resonance Raman process in the range of 2500 – 2800 cm^{-1} of the Raman spectra for crystalline graphite and is called *G′*, also reported as *2D* and D^* by some researchers [22].

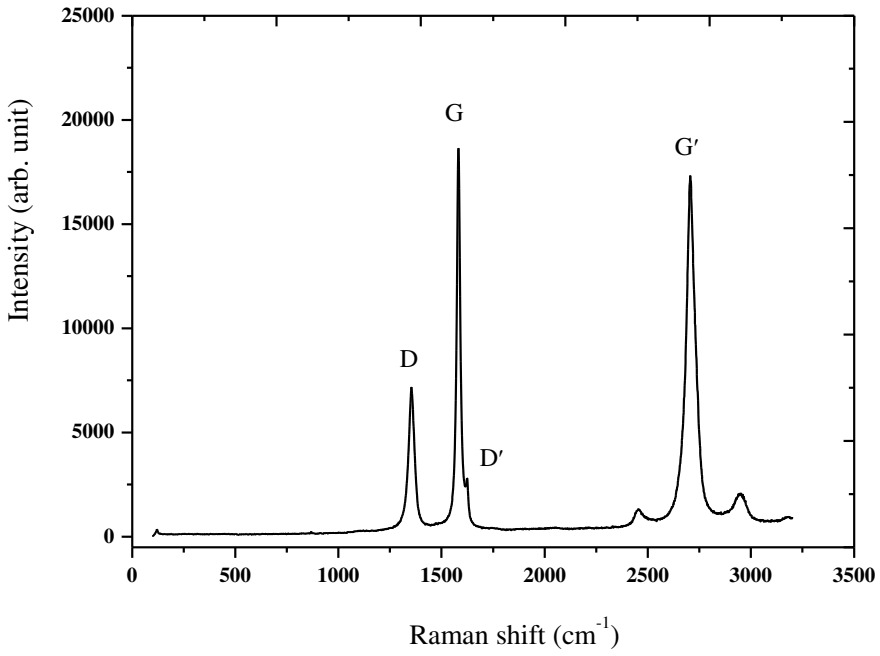

Figure 4 Raman spectrum of the graphite particle shown in Figure 1.

The intensities and wave numbers (cm^{-1}) of the *D*, *G*, *D′* and *G′* bands of this Raman spectra are given in Table 1.

Table 1 Intensities and wave numbers (cm^{-1}) of *D*, *G*, *D′* and *G′* bands of the Raman spectra shown in Figure 4.

Band	Max. Intensity (arbitrary units)	Wave number (cm^{-1})
D	**6860**	**1357**
G	**18040**	**1585**
D'	**2547**	**1626**
G'	**17320**	**2707**

As the intensity of the D band of the Raman spectra represents the defective (poorly crystalline) part of graphite, and the intensity of the G band represents the crystalline part of graphite the crystallinity of graphite can be derived from the intensity ratio of the D band to the G band (I_D/I_G) [22]. These data were thus used to calculate the *D/G* Intensity Ratio (I_D/I_G) for the Raman spectra from selected graphite particles formed from each of the starting microstructures of the experimental steel after a graphitising anneal for different time periods. Thus the spectrum analysed in Fig. 4, for the graphite particle in Fig. 1 formed in a ferrite-pearlite microstructure, showed an Intensity Ratio (I_D/I_G), calculated from the heights of the D and G bands, of 0.38. It thus appears that annealing the ferrite-pearlite microstructure in the experimental steel for 300 minutes results in highly crystallised graphite particles. This is in agreement with high-resolution TEM images reported by Inam [8].

For comparison, the value of I_D/I_G for carbon with poor crystallinity lies in the range of 1 to 2.6 with a standard deviation of 0.8 to 1.2 and for highly crystalline carbon its value is in the range of 0.1 to 0.3 with a standard deviation of up to 0.2 [22]. Walter [22] also reported that the variation in measurement of values of I_D/I_G for highly crystalline graphite is 0.4. It thus appears that annealing the ferrite-pearlite microstructure in the experimental steel for 300 minutes results in highly crystallised graphite particles.

The effect of annealing time on the extent of graphite particle crystallinity can be measured by repeating this procedure. The results are presented first for the case of martensite, mentioned already as containing the smaller particles which are more difficult to measure.

3.1 *Crystallinity of the fine graphite dispersion formed from martensite starting microstructure*

Table 2 shows the effect of annealing time on the I_D/I_G Intensity Ratio for graphite particles formed from a martensite starting microstructure.

Table 2 Effect of annealing time on the Intensity Ratio I_D/I_G of the Raman spectrum for graphite particles formed from a martensite starting microstructure.

Particle No.	I_D/I_G at Annealing Time Period (minutes)					
	20	**30**	**60**	**120**	**180**	**300**
1	3.03	1.06	0.64	0.45	0.46	0.62
2	1.15	0.57	0.66	0.58	0.38	0.41
3	0.64	3.48	--	0.38	--	0.31
4	0.60	0.31	--	0.54	--	--
5	0.58	--	--	0.36	--	--
6	0.53	--	--	0.37	--	--
Average	1.09	1.36	0.65	0.46	0.42	0.45

The values recorded in Table 2 are plotted in Figure 5. A wide range of I_D/I_G ratios, from 0.31 to 3.48, was recorded during the early stages of graphitisation, after 20 and 30 minutes of annealing, suggesting that the graphite particles examined had widely different degrees of crystallinity, probably resulting from their nucleation at different time periods during the annealing treatment. This is the most likely explanation for the higher value for I_D/I_G of 3.48 observed after 30 minutes of annealing. After 60 minutes of graphitising anneal, the I_D/I_G ratios measured had decreased closer to ~0.65 revealing a more consistent general increase of crystallinity.

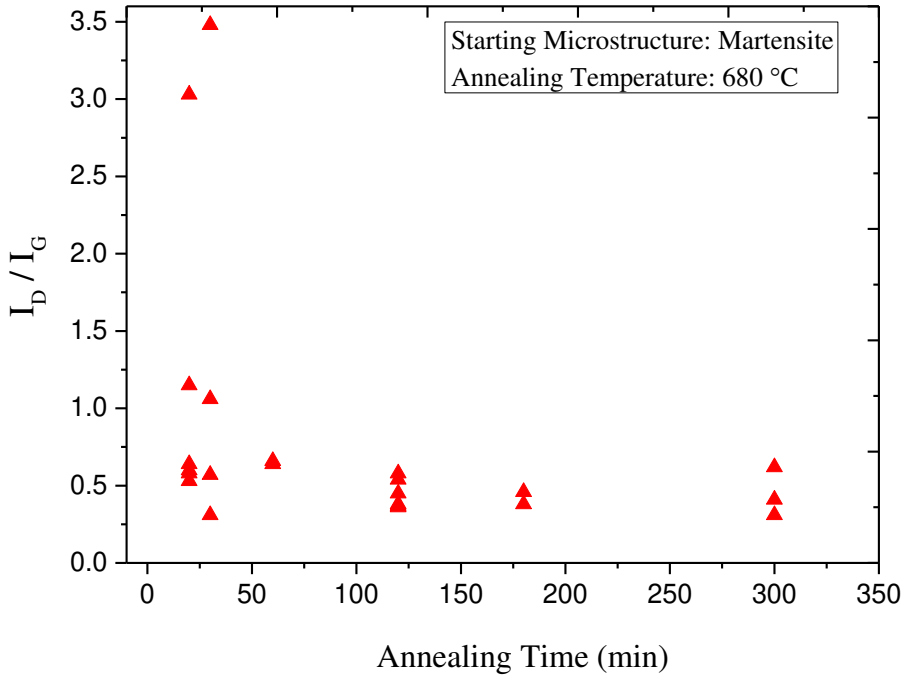

Figure 5 Effect of annealing time on I_D/I_G as recorded in Table 2 for graphite particles formed from martensite starting microstructure.

After annealing for longer periods the spread of data across the particles examined narrowed further. Thus, after 120 minutes of graphitising anneal, the mean value of I_D/I_G was ~ 0.45, which remained virtually unchanged up to 300 minutes, suggesting little further improvement in crystallinity.

3.2 *Crystallinity of a medium graphite dispersion formed from bainite starting microstructure*

Table 3 shows the effect of annealing time on the I_D/I_G Intensity Ratio for graphite particles formed from a bainite starting microstructure.

Table 3 Effect of annealing time on the Intensity Ratio I_D/I_G of the Raman spectrum of graphite particles formed from bainite starting microstructure.

Particle No.	I_D/I_G at Annealing Time Period (min)					
	20	30	60	120	180	300

1	1.71	0.50	0.40	0.41	0.57	0.48
2	0.56	0.63	0.49	0.34	0.47	0.52
3	0.50	--	0.36	0.49	0.42	0.44
4	0.41	--	--	0.35	0.69	0.45
5	0.82	--	--	--	0.47	0.63
6	2.18	--	--	--	--	--
Average	1.03	0.57	0.42	0.40	0.52	0.50

The values given in Table 3 are plotted in Figure 6. Higher values of I_D/I_G up to 2.18 as well as lower values were observed after 20 minutes of graphitising anneal, again suggesting various levels of crystallinity developed in the early stages of graphite dispersion formation.

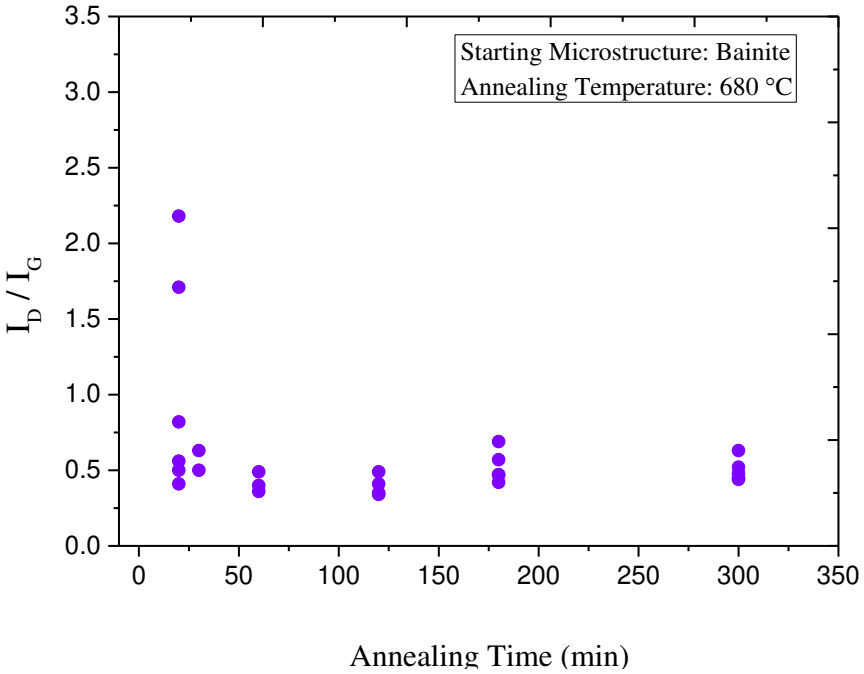

Figure 6 Effect of annealing time on I_D/I_G as recorded in Table 3 for graphite particles formed from bainite starting microstructure.

After 30 and 60 minutes of graphitising anneal, although data were limited, the value and spread of the I_D/I_G values reduced, indicating an improvement in crystallinity. In addition, as

for martensite, there was little further change after 180 minutes (mean 0.52) and 300 minutes (mean 0.50) of annealing. This similarity in behaviour of the less-refined graphite particles compared to the martensite microstructure suggests that the Raman spectra from the finer particles in martensite were satisfactorily recording the correct behaviour during annealing.

3.3 *Crystallinity of coarse graphite dispersion formed from ferrite-pearlite starting microstructure*

Table 4 shows the effect of annealing time on the I_D/I_G Intensity Ratio for graphite particles formed from a ferrite-pearlite starting microstructure.

Table 4 Effect of annealing time on the Intensity Ratio I_D/I_G of the Raman spectrum for graphite particles formed from ferrite-pearlite starting microstructure.

Particle No.	I_D/I_G at Annealing Time Period of (min)					
	20	**30**	**60**	**120**	**180**	**300**
1	0.47	0.46	0.51	0.35	0.35	0.45
2	0.56	0.35	0.34	0.39	0.44	0.38
3	0.66	0.39	0.45	0.32	0.47	0.31
4	0.45	0.45	0.30	0.33	0.34	0.46
5	--	0.51	--	--	--	0.31
Average	0.53	0.43	0.40	0.35	0.40	0.38

The values given in Table 4 are plotted in Figure 7. More data was collected for this microstructure at each annealing time. It was noted that the martensite and bainite microstructures were fully graphitized after 30 minutes of annealing, while the ferrite-pearlite microstructure was fully graphitized only after 4 hours of annealing, also consistent with the previous detailed microstructural characterisation by Inam et al. [8, 9,12]. Interestingly, this revealed no high values of I_D/I_G even for the shorter annealing times, unlike the martensite and bainite starting microstructures.

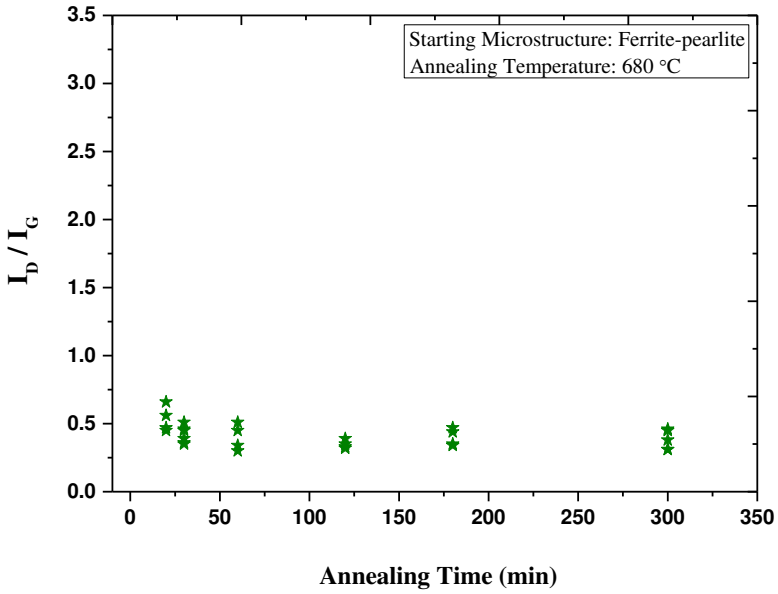

Figure 7 Effect of annealing time on I_D/I_G as recorded in Table 4 for graphite particles formed from ferrite-pearlite starting microstructure.

A maximum I_D/I_G value of 0.66 and mean value of 0.54 were recorded after the 20 minute anneal, after which little change was observed up to 300 minutes. It was also noticed that, in general, the minimum and mean I_D/I_G values of graphite particles formed from ferrite-pearlite starting microstructure were lower than those for the other two starting microstructures. This suggests that the graphite particles formed from a ferrite-pearlite starting microstructure nucleated and crystallised more rapidly in comparison with those formed from the martensite and bainite starting microstructures. It is thus possible that the extent of graphite crystallinity, here dependent upon the starting microstructure, could be influential on its dry lubrication potential, and thus contribute to machinability dependent upon optimising the heat treatment and base microstructure.

The average values of I_D/I_G from the Raman spectra of graphite particles formed from martensite, bainite and ferrite-pearlite starting microstructures as given in Table 2, 3 and 4, respectively, are plotted against the annealing period in Figure 8.

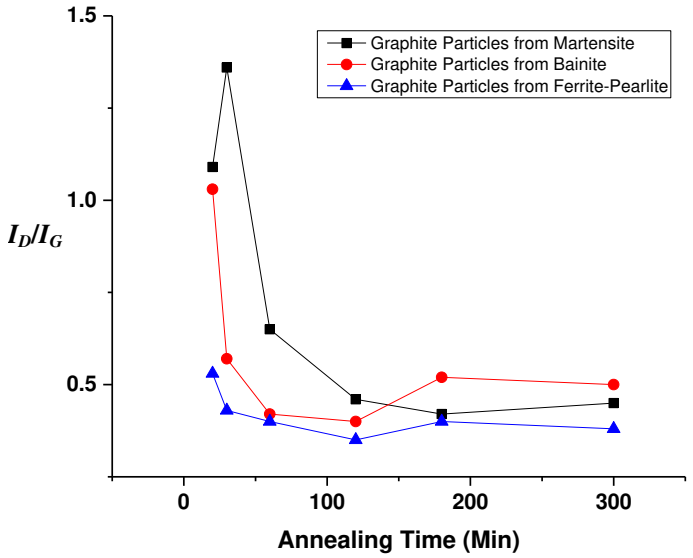

Figure 8 Average values of I_D/I_G from Raman spectra of graphite particles formed from starting microstructures; martensite, bainite and ferrite-pearlite plotted against graphitising anneal times (20—300 min).

The average values of I_D/I_G from the Raman spectra obtained revealed that higher values of intensity ratio were observed from graphite particles formed in the martensite and bainite microstructures, while ferrite-pearlite microstructure resulted in lower values of I_D/I_G ratio. The I_D/I_G ratio, after an initial rapid drop, generally continued to decrease at a lower rate for all the microstructures, apart from the behaviour of the bainite at the longer time periods shown by this set of measurements. This is consistent with the suggestion that the starting microstructure has a strong influence on the crystallinity of the graphite particles. The graphitising anneal time period also appeared to affect the crystallinity at the start of the process but thereafter, according to this set of measurements, crystallinity was virtually unaffected by increasing anneal time.

Conclusions

The crystallinity of graphite particles formed by high temperature annealing of various microstructures in a carbon steel has been examined and measured by Raman spectroscopy. Starting microstructures of ferrite-pearlite, bainite and martensite were studied. Higher values of the I_D/I_G Intensity Ratios of the Raman spectra obtained from the more refined dispersions of graphite particles formed in the bainite and martensite starting microstructures observed after 20 minutes of annealing revealed poor crystallinity. With an increase of annealing times

up to 300 minutes the I_D/I_G values decreased consistently, indicating improving crystallinity. In comparison, the coarser graphite particles formed from ferrite-pearlite starting microstructure showed lower I_D/I_G Intensity Ratios in the early stage, after only 20 minutes of annealing, indicating that already very good crystallinity had been achieved. In consequence, further increase in annealing time up to 300 minutes showed only a slight lowering of I_D/I_G. The difference in graphite phase crystallinity reflects the differences in the graphite formation process between the starting microstructures, particularly confirming the importance of the availability and distribution of the initial cementite dispersion as a potential heterogeneous nucleation site as well as a concentrated source of carbon. In this respect the results of the Raman study mirror those emerging from other studies using high resolution electron microscopy, whilst also providing relatively easily and quickly, comprehensive information on the degree of graphitisation as a function of microstructure and heat treatment, which may contribute towards the final overall behaviour of the steel.

Acknowledgements

We are grateful to Tata Steel, Rotherham, UK, for providing the experimental steel for this investigation. Aqil Inam is also indebted to the University of the Punjab, Lahore, Pakistan for financial support whilst undertaking this research.

References

[1] T. Iwamoto, T. Hoshino, K. Amano, Y. Nakano, An advanced high strength graphitised steel for machining and cold forgings uses, in: C.J. Van Tyne, G. Krauss, D.K. Matlock (Eds.), Fundamentals and Applications of Microalloying Forging Steels, TMS/Minerals, Metals and Materials Society, Warrendale, PA, 1996, pp. 277-286.

[2] E. M. Trent, P.K. Wright, Metal Cutting, 4th ed. Butterworth-Heinemann, Boston, 2000.

[3] T.H.C. Childs, K. Maekawa, T. Obikawa, Y. Yamane, Metal Machining: Theory and Applications, Arnold, London, 2000.

[4] T. Akasawa, H. Sakurai., M. Nakamura, T. Tanaka, K. Takano, Effects of free-cutting additives on the machinability of austenitic stainless steels, Mater. Proc. Technol. 143-144 (2003) 66─71.

[5] K. He, D.V. Edmonds, A potential graphitisation route to improved machinability of carbon steels, International Conference on New Developments in Long and Forged Products: Metallurgy and Applications, , June 4-7, Winter Park, Colorado, USA, Association for Iron & Steel Technology AIST, 2006, pp. 49-56.

[6] K. He, A. Brown, R. Brydson, D.V. Edmonds, Analytical electron microscope study of the dissolution of the Fe_3C iron carbide phase (Cementite) during a graphitisation anneal of carbon steel, J Mater. Sci. 41 (2006) 5235-5241.

[7] K. He, H.R. Daniels, A. Brown, R. Brydson, D.V. Edmonds, An electron microscopic study of spheroidal graphite nodules formed in a medium-carbon steel by annealing, Acta Mater. 55 (2007) 2919─2927.

[8] A. Inam, Machinability of Graphitised Carbon Steel, PhD Thesis, University of Leeds, UK, 2013.

[9] A. Inam, R. Brydson, D.V. Edmonds, Effect of starting microstructure upon the nucleation sites and distribution of graphite particles during a graphitising anneal of an experimental medium-carbon machining steel, Mater. Charact. 106 (2015) 86─92.

[10] D.V. Edmonds, R. Brydson, A. Inam, High-resolution metallography of a coarse microstructure: Graphite formation in the solid-state in steel, Mater. Perf. and Charact. 5 (5) (2016) 780─795.

[11] A. Inam, K. He, D.V. Edmonds, Graphitisation: A potential new route to free-machining steels, HSLA Steels 2015: Microalloying 2015 and Offshore Engineering Steels 2015, Hangzhou, China, November 2015. The Chinese Society for Metals and Chinese Academy of Engineering, Wiley TMS, 2016, pp. 817-822.

[12] A. Inam, R. Brydson, D.V. Edmonds, A high-resolution study of graphite nodule formation in experimental medium-carbon machining steel, Mater. Charact. 131 (2017) 508─516.

[13] J.X. Gao, B.Q. Wei, D.D. Li, K. He, Nucleation and growth characteristics of graphite spheroids in bainite during graphitisation annealing of a medium carbon steel, Mater. Charact. 118 (2016) 1–8.

[14] T. Iwamoto, T. Murakami, Bar and wire steels for gears and valves of automobiles - Eco-friendly free cutting steel without lead addition, JFE, Osaka, Japan, Technical Report No. 4, (2004) 64─69.

[15] J. R. Foulds, V. Viswanathan, Graphitization of steels in elevated-temperature service, J. Mater. Eng. Perform. 10 (2001) 484─492.

[16] K. Banerjee, T. Venugopalan, Development of hypo-eutectoid graphitic steel for wires, Mater. Sci. Technol. 24 (2008) 1174─1178.

[17] K. Oikawa, T. Abe, S. Sumi, Medium-carbon Steel Having Dispersed Fine Graphite Structure and Method for the Manufacture Thereof, Patent 6174384, United States of America (2001).

[18] S. Katayama, T. Tarui, M. Toda, K. Naito, Fine Graphite Uniform Dispersion Steel Excellent in Cold Machinability, Cuttability and Hardenability, and Production Method for the Same, Patent 5830285, United States of America (1998).

[19] D. Li, R. Tan, J. GaO, B. Wei, Z. Fan, Q. Huang, K. He, Comparison of pyrolytic graphite spheres from propylene with spheroidal graphite nodules in steel, Carbon 111 (2017) 428─438.

[20] Q. Wang, D.D Allred, Low-frequency feature in the first-order Raman spectrum of amorphous carbon, Phys. Rev. B. 47 (1993) 6119─6121.

[21] M. Tommasini, C. Castiglioni, G. Zerbi , A. Barbon, M. Brustolon, A joint Raman and EPR spectroscopic study on ball-milled nanographites, Chem. Phys. Lett. 516 (2011) 220─224.

[22] J. M. Walter, Raman Spectroscopy of Graphite, 2013, https://jumwalter.de/plaintext/geo-und-mehr/raman-spectroscopy-of-graphite.html